

# STUDIES ON CHARACTERIZATION OF SODIUM FLUORO ANTIMONATE CRYSTALS GROWN BY SOLUTION METHOD

R.Kumuthini<sup>1</sup>, P.Selvarajan<sup>2</sup>, S.Selvaraj<sup>1</sup>

<sup>1</sup> PG and Research Centre, Department of Physics, MDT Hindu College, Tirunelveli-627010, India.

<sup>2</sup>Department of Physics, Aditanar College of Arts and Science,  
Tiruchendur-628216, India

**Abstract** - Single crystals of sodium fluoro antimonate ( $\text{Na}_3\text{Sb}_4\text{F}_{15}$ ) were grown by slow evaporation technique for the first time. The solubility of the crystal in water has been studied. The mechanical properties and work hardening coefficient of the grown crystal has been studied using Vickers microhardness tester. The etch patterns of the grown crystals were studied. The grown crystals were characterized with the aid of single crystal X-ray diffractometry to confirm the crystal structure. The vibrational frequencies of various group ligands in the crystal have been derived from the Fourier transform infrared (FT-IR) spectrum. Thermal stability of the sample has been analysed using TG-DTA studies. The dielectric constant ( $\epsilon_r$ ) and dielectric loss ( $\tan \delta$ ) were determined as a function of frequency in the range 100 Hz-200 kHz at different temperatures between 40°C- 150°C.

## 1. INTRODUCTION

Studies on the crystal chemistry of fluoro antimonates and their related compounds have been reported in literature [1-5]. It has also been reported that a number of fluorides have high ionic conductivity. Ammonium penta fluoro di antimonate,  $(\text{NH}_4)_2\text{SbF}_4$ , has shown superionic conductivity [6], and it is reported that the phase transitions are at 257 K and 398 K and the successive phase transitions are due to the reorientations of  $\text{NH}_4^+$  and  $[\text{SbF}_5]^{2-}$  groups. The potassium fluoro antimonates  $\text{KSbF}_4$  and  $\text{K}_3\text{Sb}_4\text{F}_{15}$  are observed to be showing high ionic conductivity [7]. Dielectric measurements of grown single crystals of  $\text{Na}_2\text{SbF}_5$  and  $\text{Na}_3\text{Sb}_2\text{F}_9$  have been carried out [8]. Growth and microhardness studies of  $\text{NaSbF}_4$ ,  $\text{NaSbF}_5$ ,  $\text{NaSb}_2\text{F}_7$  and  $\text{Na}_3\text{Sb}_2\text{F}_9$  have been reported in the literature [9]. Growth, microhardness and correction to the diagonal length of the indentation impression of  $\text{Na}_2\text{SbBF}_8$  crystals have been reported by Benet Charles *et al.* [10]. Dislocation studies by chemical etching on solution grown  $\text{NaSbF}_4$  single crystals were reported in the literature [11]. X-ray and electrical characterization of  $\text{NaSb}_2\text{F}_7$  single crystals were reported by Sivakumar *et al.* [12]. The aim of this paper is to report the growth and characterization of sodium fluoro antimonate ( $\text{Na}_3\text{Sb}_4\text{F}_{15}$ ) crystals.

## 2. EXPERIMENTAL PROCEDURE

### 2.1 GROWTH OF SODIUM FLUORO ANTIMONATE CRYSTALS

Sodium fluoride, antimony trioxide and hydrofluoric acid were used as the starting materials for the preparation of  $\text{Na}_3\text{Sb}_4\text{F}_{15}$  sample. These materials were dissolved in double distilled water as per the chemical equation given below.



The saturated solution was kept in a hot water bath to obtain super saturated solution and was kept in a constant temperature bath at 305 K for the growth crystals. The seed crystals were prepared by spontaneous nucleation. The crystals were grown by slow and controlled evaporation of the solvent in the constant temperature bath. Single crystals of sodium fluoro antimonate ( $\text{Na}_3\text{Sb}_4\text{F}_{15}$ ) with the dimensions upto 18 x 12 x 8 mm<sup>3</sup> have been grown over a period of 1 month. A harvested crystal of  $\text{Na}_3\text{Sb}_4\text{F}_{15}$  is shown in the figure 1. It is observed that the grown crystal is transparent, non-hygroscopic and colourless.

### 2.2 CHARACTERIZATION TECHNIQUES

The single crystal XRD data of the  $\text{Na}_3\text{Sb}_4\text{F}_{15}$  single crystals are obtained to find the lattice dimensions using ENRAF NIUS CAD-4 X-ray diffractometer. The powder XRD data of  $\text{Na}_3\text{Sb}_4\text{F}_{15}$  powder are obtained using a SIEFERT X-ray diffractometer. The powdered sample was scanned in steps of 0.02° for a time interval of 2 s over a 2-theta range of 10-70°. The mechanical properties of the grown crystals are studied using a SHIMADZU HMV-2000 micro hardness tester fitted with a Vickers diamond pyramid indenter. The micro hardness number ( $H_v$ ) of the material is determined by the relation,  $H_v = 1.8544 P/d^2$  kg/mm<sup>2</sup>, where P is the load applied in grams and d is the diagonal length of the indentation impression in mm [13]. Thermal behavior of the crystal of  $\text{Na}_3\text{Sb}_4\text{F}_{15}$  was studied by analyzing the TG/DTA thermal curves recorded using the instrument Perkin Elmer thermal analyzer in nitrogen atmosphere at a heating range of 5°C to 700°C. Dielectric studies of the sample have been carried out at different frequencies and temperatures using a HIOKI 3532 LCR Hitester with a conventional two terminal sample holder.

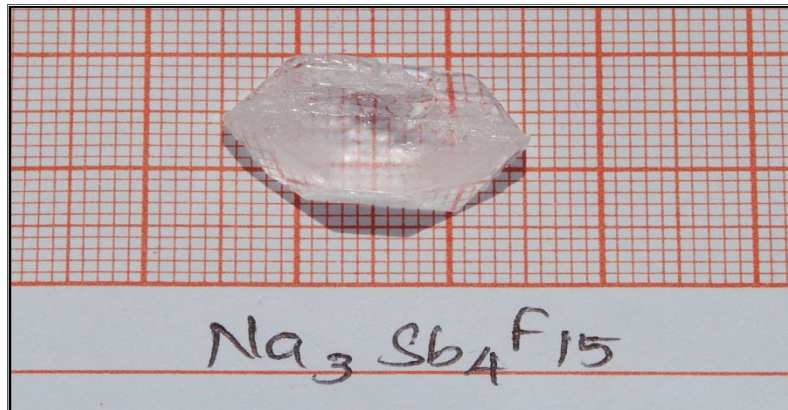


Fig.1: A grown crystal of sodium fluoro antimonate

Etching studies of the grown crystal were performed using a metallurgical-optical microscope with polarizing facility gets light from halogen lamp.

### 3. RESULTS AND DISCUSSION

#### 3.1 Solubility studies

The solubility of the crystal of  $\text{Na}_3\text{Sb}_4\text{F}_{15}$  was measured in the temperature range 30-60 °C. A volume of 100 ml of water was taken in a container and re-crystallized salt was added. The temperature of the solution was maintained above the chosen constant temperature and continuously stirred using a magnetic stirrer to ensure homogeneous temperature and concentration throughout the entire region of the solution. Once the saturation was reached, the equilibrium concentration of the solute was analyzed gravimetrically [14]. The experiment was carried out for various temperatures from room temperature to 60 °C in steps of 10°C and the solubility curve was drawn and it is presented in the Fig.2. The solubility curve indicates that  $\text{Na}_3\text{Sb}_4\text{F}_{15}$  crystal has positive temperature coefficient of solubility. Fig.2 shows three regions viz. saturation region is along the solubility curve, super saturation region is above the solubility curve and under saturation region is below the solubility curve. Using these results, the saturated and saturated solutions of the sample could be prepared at a particular temperature and nucleation kinetic studies and growth of crystals can be carried out.

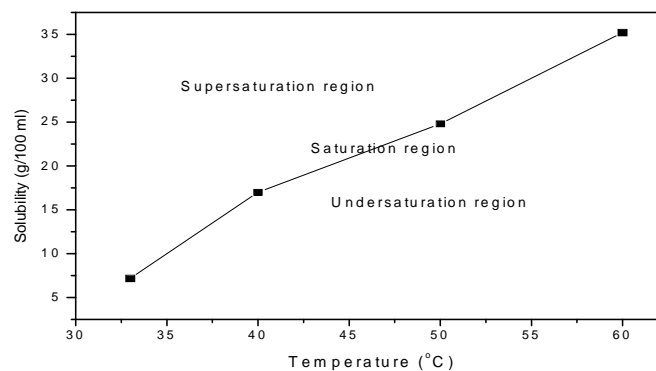


Fig.2: Solubility curve of  $\text{Na}_3\text{Sb}_4\text{F}_{15}$  crystal

#### 3.2 XRD STUDIES

Single crystal and powder XRD studies have been carried out for the grown crystals of  $\text{Na}_3\text{Sb}_4\text{F}_{15}$  to find the crystal structure and diffraction planes. From the single crystal X-ray diffraction analysis, it is found that the  $\text{Na}_3\text{Sb}_4\text{F}_{15}$  crystal crystallizes in monoclinic system with lattice parameters  $a = 8.131(2) \text{ \AA}$ ,  $b = 5.494(1) \text{ \AA}$ ,  $c = 8.652(3) \text{ \AA}$ ,  $\alpha = 90^\circ$ ,  $\beta = 94.37^\circ$ ,  $\gamma = 90^\circ$ , and volume of the unit cell,  $V = 385.41(2) \text{ \AA}^3$ . The powder X-ray powder diffraction analysis was carried out to find the diffraction planes and to confirm the identity of the grown crystal. To prepare powder sample for XRD, the as-grown crystal of  $\text{Na}_3\text{Sb}_4\text{F}_{15}$  were ground using agate mortar and pestle. The XRD pattern of crystal of  $\text{Na}_3\text{Sb}_4\text{F}_{15}$  was recorded on a microprocessor controlled X-ray diffractometer (SIEFERT XRD 3000P) using nickel filtered  $\text{CuK}_\alpha$  radiation. The powder XRD pattern of  $\text{Na}_3\text{Sb}_4\text{F}_{15}$  sample is given in Fig.3. From the X-ray diffraction spectrum, the two theta ( $2\theta$ ) values were read directly and the relative intensities of the diffraction peaks were estimated. The d-spacings corresponding to different peak positions were obtained by default calculation using the Bragg's relation  $2d \sin \theta = n \lambda$  where  $d$  is the inter-planar spacing,  $\theta$  is the Bragg's angle,  $n$  is the order of diffraction and  $\lambda$  is the wavelength of X-rays. When X-rays penetrate through the powdered sample, a number of particles can be expected to be oriented in such a way as to satisfy the Bragg's condition for reflection from every possible inter planar spacing. The reflections of the XRD pattern were indexed using the INDEXING software package.

The powder XRD data for the sample are given in the table 1. Using the powder XRD data, the unit cell parameters of sodium fluoro antimonate crystal have been evaluated using the UNITCELL software package. The obtained lattice constants from powder XRD studies are  $a = 8.132 \text{ \AA}$ ,  $b = 5.492 \text{ \AA}$ ,  $c = 8.650 \text{ \AA}$ ,  $\alpha = 90^\circ$ ,  $\beta = 95.02^\circ$ ,  $\gamma = 90^\circ$ . It is observed that the lattice constants obtained from single crystal XRD studies and powder XRD studies are almost the same.

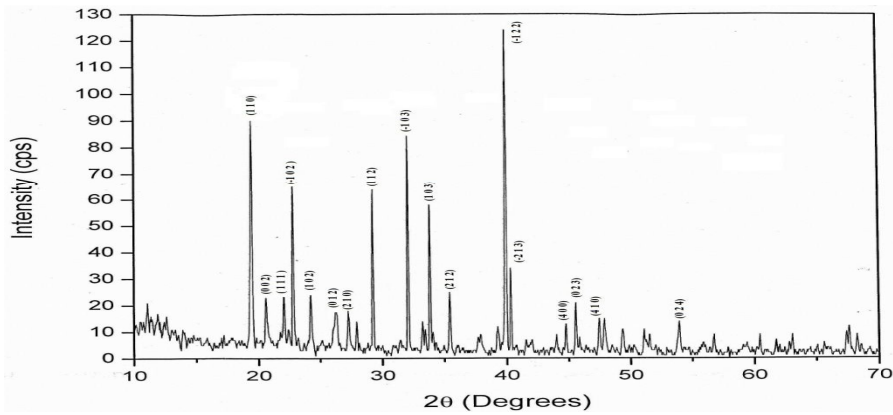


Fig.3: Powder XRD pattern of sodium fluoro antimonate crystal

TABLE 1: POWDER XRD DATA FOR SODIUM FLUORO ANTIMONATE SAMPLE

Peak No	2 $\theta$ (degrees)	$d_{hkl}$ ( $\text{\AA}$ )	h	k	l	Relative intensity(%)
1.	19.50	4.55	1	1	0	73.6
2.	20.57	4.31	0	0	2	19.2
3.	22.47	3.95	1	1	1	20.0
4.	22.58	3.93	-1	0	2	51.2
5.	24.08	3.69	1	0	2	20.8
6.	26.25	3.39	0	1	2	14.4
7.	27.32	3.26	2	1	0	14.4
8.	29.11	3.07	1	1	2	51.2
9.	32.20	2.78	-1	0	3	67.2
10.	33.83	2.65	1	0	3	44.0
11.	35.48	2.53	2	1	2	20.0
12.	39.99	2.25	-1	2	2	100.0
13.	40.49	2.23	-2	1	3	27.4
14.	44.67	2.03	4	0	0	10.4
15.	45.63	1.99	0	2	3	16.0
16.	47.80	1.90	4	1	0	11.2
17.	54.01	1.70	0	2	4	10.4

### 3.3 FT-IR ANALYSIS

Infrared absorption studies are important in the investigation of molecular structure of crystals. This study involves examination of stretching, bending, twisting and rotating vibrational modes of atoms in a molecule and hence to identify the functional groups of samples. When infrared radiation interacts with a sample, a portion of the incident radiation is absorbed at a specific wavelength. The FT-IR spectrum of the sample were recorded using a Perkin-Elmer FT-IR spectrometer using KBr pellet technique in the range  $4000-400 \text{ cm}^{-1}$  and it is presented in the figure 4. The broad vibrational band observed around  $3444 \text{ cm}^{-1}$  is attributed to asymmetric OH stretching mode of adsorbed water molecule in the sample. The medium broad band noticed around  $1632 \text{ cm}^{-1}$  is assigned to the bending vibration of water molecules. The assignments for peaks/bands are given in accordance with the data in the literature [15]. The FT-IR assignments for the absorption peaks/bands of the sample are provided in the table 2.

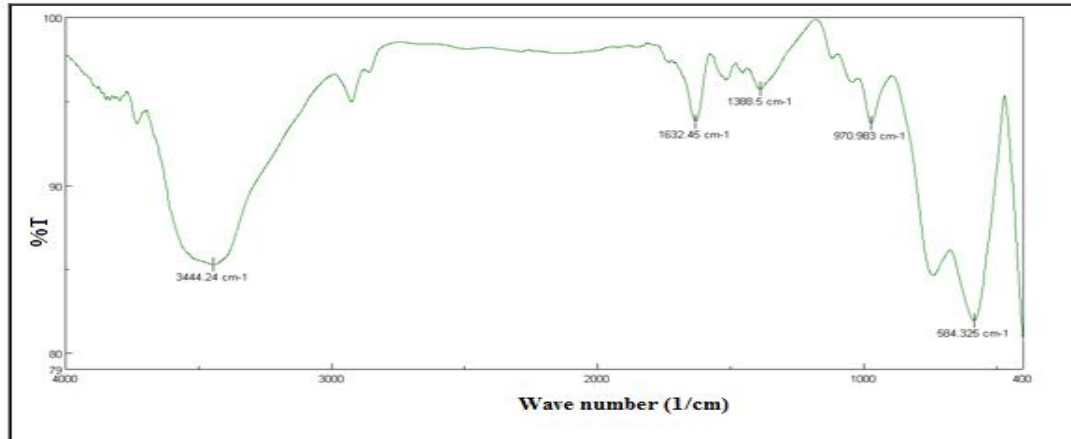


Fig.4: FTIR spectrum of sodium fluoro antimonate crystal

Table 2: FTIR assignments for sodium fluoro antimonate crystal

Wave number (cm <sup>-1</sup> )	Assignments
3444.24	O-H stretching mode of adsorbed water molecule
1632.45	O-H bending mode
970.983	Sb-F vibration
584.325	Sb-F bending mode

### 3.4. THERMAL ANALYSIS

TG/DTA thermal curves for sodium fluoro antimonate crystal were recorded using a TG/DTA thermal analyzer in the temperature range 30-700 °C and it is shown in the figure 5. It is clear from the TG curve that the sample is thermally stable upto 260 °C. The sample undergoes endothermic transition at 264 °C and it corresponds to melting point of the sample. At this temperature, there is a slight weight loss of about 5 weight % and it may be due to the adsorbed water molecules. It may be noted here that the endothermic transition at 264 °C is not the decomposition point because there is no heavy weight loss of the sample. The sharp endothermic peak shows the good crystalline perfection of the sample. When the temperature is increased above the melting point, there is a gradual and significant weight loss (75%) occurs in the range of temperature 270-650 °C and this is due to the decomposition and the release of gaseous particles such as fluorine and other ions from the lattice of the crystal. The DTA curve also shows the same kind of thermal transitions in the sample.

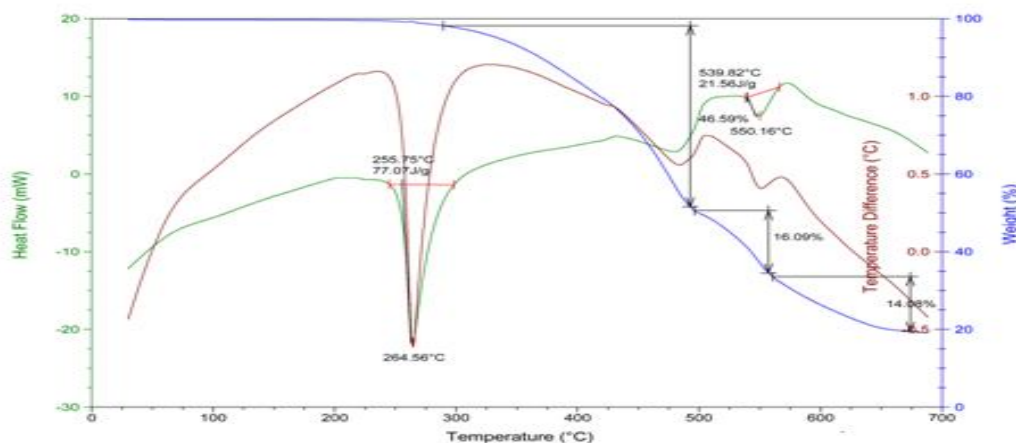


Fig.5: TG/DTA thermal curves for the sodium fluoro antimonate

### 3.5. MICROHARDNESS STUDIES

Hardness is one of the important mechanical properties of solid material. It can be used as a suitable measure of the plastic properties and strength of the material. Microhardness testing is one of the best methods of understanding the mechanical properties of materials such as fracture behavior, yield strength, brittleness index and temperature of cracking [16]. Transparent crystals free from cracks were selected for microhardness measurements. Before indentations, the crystals were carefully lapped and washed to avoid surface effects. Microhardness analyses were carried out using Shimadzu Vickers microhardness tester fitted with a diamond indenter attached to an incident light microscope.

The well polished sodium fluoro antimonate crystal was placed on the platform of the Vickers microhardness tester and the loads of different magnitude were applied over a fixed interval of time. The indentation time was kept as 10 sec for all the loads. As given in the section 2.2, the microhardness number was determined using the relation  $H_v = 1.8544 P/d^2$ . The variation of hardness number with the applied load for the sample is shown in the figure 6. The results show that hardness number increases gradually upto 20 grams and then it decreases and this indicates that the sample could withstand the weight upto 20 grams. The increasing part of the curve is due to the reverse indentation size effect and the decreasing part of the curve is due the direct indentation size effect.

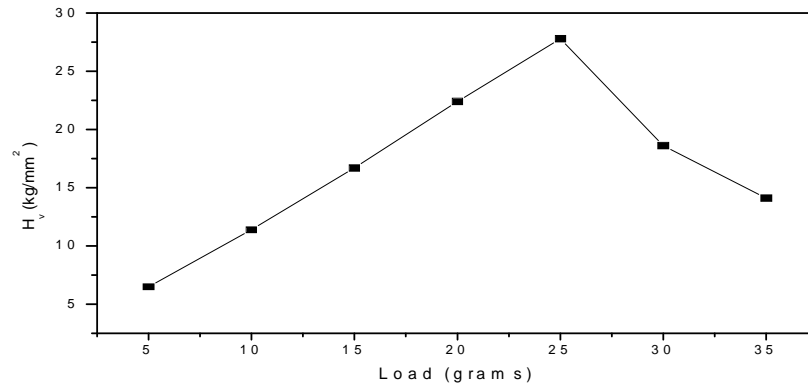


Fig.6: Variation of hardness number with applied load for sodium fluoro antimonate

### 3.6. ETCHING STUDIES

The etching studies reveal the structural perfection and growth features of grown single crystal of sodium fluoro antimonate. Transparent single crystal of  $Na_3Sb_4F_{15}$  was etched in distilled water for 5 s, 15 s and 25 s. Leitz optical microscope was used to study the etched faces. The etched samples were dried using a tissue paper and surface features were analyzed using the optical microscope. The sample is magnified by the objective which has magnification from 10 to 150 times. The magnified image is viewed through the eyepieces which have magnification from 8 times to 20 times. The etching patterns of the sample are presented in the figures 7 (a), (b) and (c). The results show that when the sample is etched for 5 seconds, it does not reveal the pyramidal shaped etch pits. But when the sample is etched with water for 15 seconds and 25 seconds, it shows pyramidal shaped etch pits.

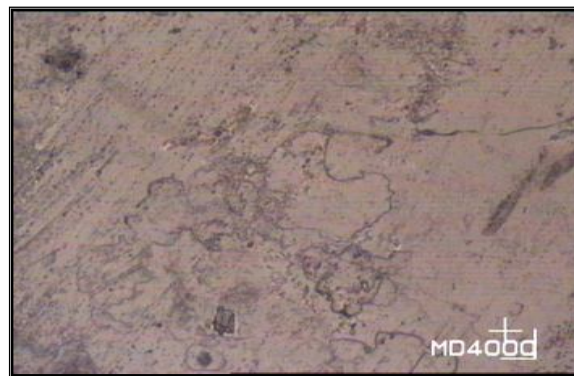


Fig.7(a)

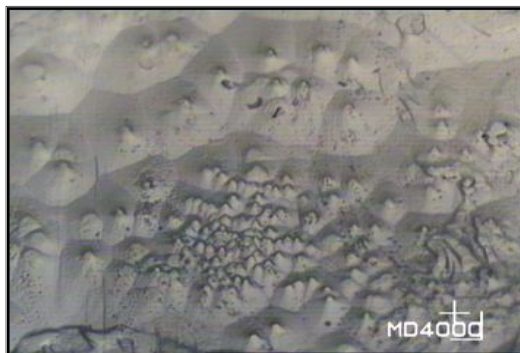


Fig.7(b)

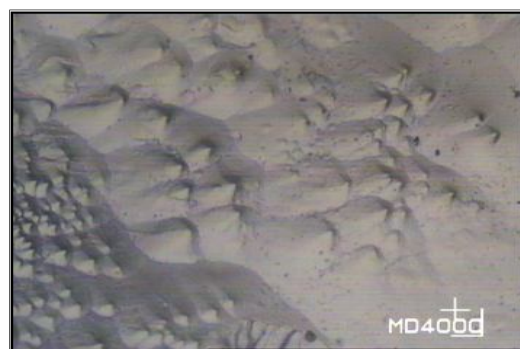


Fig.7 (c)

Fig.7 Etching patterns of the sample: (a) etched for 5 seconds, (b) etched for 15 seconds and (c) etched for 25 seconds

### 3.7 DIELECTRIC STUDIES

A study of dielectric response in crystals is one of the basic electrical properties which give the information about the electric field distribution within the solid. Crystals with high transparency and defect free are selected and used for the dielectric measurements. The extended portion of the crystal is removed completely and the opposite faces are polished and coated with good quality graphite to obtain a good ohmic contact. The dielectric constant ( $\epsilon_r$ ) is calculated using the relation  $\epsilon_r = (C d) / (\epsilon_0 A)$  where C is the capacitance, d is the thickness of the sample, A is the area of the electrode contact and  $\epsilon_0$  is the absolute permittivity of the free space. The dielectric loss of the sample was directly measured using the LCR meter. Figures 8 and 9 show the variations of dielectric constant and loss factor with temperature at different frequencies of 100 Hz, 1000 Hz, 10 kHz, 100 kHz and 200 kHz. It is seen from the plots that the dielectric constant is relatively high in the lower frequency region and then decreases with the applied frequency. The high values of dielectric constant at low frequencies may be due to the presence of combinations of all four polarizations namely space charge, orientational, electronic and ionic polarizations. The low value of dielectric constant at high frequencies occurs due to the loss of these polarizations at low temperature. Increase of dielectric constant with temperatures may be due to the thermal excitation of atoms about their lattice point and blocking of charge carriers at the electrodes [17,18].

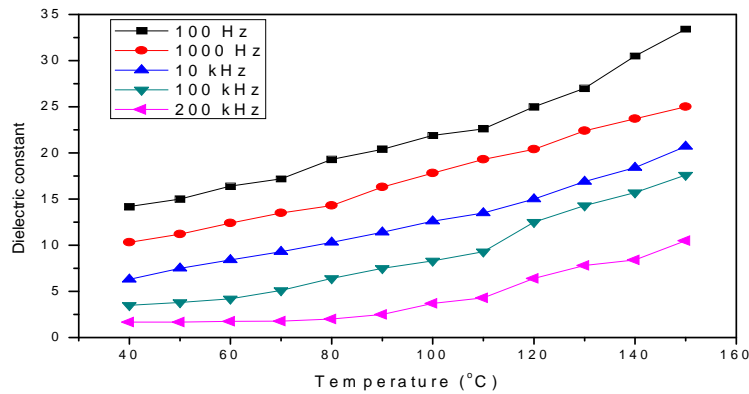


Fig.8: Variation of dielectric constant with temperature at different frequencies for sodium fluoro antimonate crystal

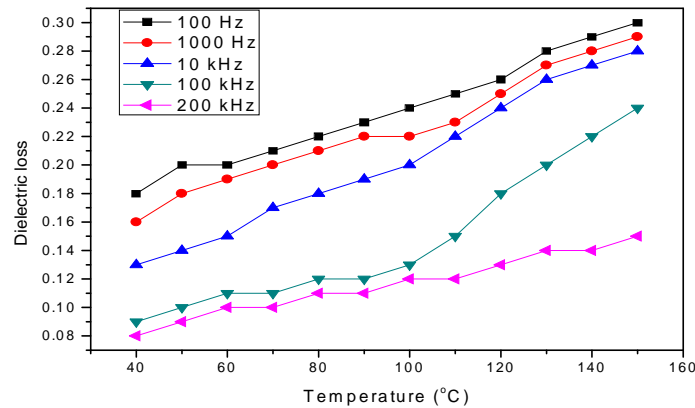


Fig.9: Variation of dielectric loss with temperature at different frequencies for sodium fluoro antimonate crystal

### 4. CONCLUSIONS

Single crystals of sodium fluoro antimonate were grown by solution growth method. The grown crystals are transparent with well defined external appearance. The solubility of the sample was determined at different temperatures by gravimetric method. The unit cell parameters have been evaluated by the single crystal and powder XRD methods. The functional groups of the grown crystals have been identified by FTIR technique. The thermal and mechanical stability of the grown sodium fluoro antimonate were studied. Etching studies reveal that the sample has pyramidal shaped etch pits. Dielectric constant and dielectric loss factor of the sample are observed to be decreasing with increase of frequency and increasing with increase of temperature.

### ACKNOWLEDGEMENT

The authors like to thank the staff members of St. Joseph's College (Trichy, India), Madras University (Chennai), IIT (Chennai, India), who helped us in many ways to complete this work. We also thank the management of Aditanar College of Arts and Science, Tiruchendur and MDT Hindu College, Tirunelveli for the encouragement and support given to carry out this work.

## REFERENCES

- [1]. J.G.Bergman, D.S.Chemla, R.Fourcade and G.Mascherba, *J.Solid State Chem.*, 23(1978) 187.
- [2]. M.B.Ducourant, B.Bonnet, R.Fourcade and G.Mascherba, *Bull.Soc.Chem.*, 8 (1975) 1471
- [3]. S.E.Gugasyan, V.P.Gorkov, L.A.Sodokhina, F.Kh.Chibirov and V.S.Shpinel, *Zh.Strukt.Khim.*, 16 (1975) 207
- [4]. Yu.Ya.Kharitonov, R.L.Davidovich, V.I.Kostin, L.A.Zemnukhova and V.I.Sergienko, *Russ.J.Inorg.Chem.*,17 (1972) 682.
- [5]. F.B.Kalinchenko, M.P.Borzenkova and A.V.Novoselova, *Russ.J.Inorg.Chem.*, 27(1982)1653
- [6]. L.M.Avkhutskii, R.L.Davidovich, L.A.Zemnukhova, P.S.Gordienko, V.Urhonevicius and J.Grigas, *Phys.Status Solidi (a)*, 116 (1983) 483
- [7]. M.V.Borzenkova, F.V.Kalinchenko, A.V.Novoselova, A.K.Ivanovshits and N.I.Sorokin, *Russ.J.Inorg.Chem.*, 29 (1984) 405.
- [8]. J.Benet Charles and F.D.Gnanam, *Cryst.Res.Technol.*, 29 (1994) 707.
- [9]. J.Benet Charles, *Studies on Growth on Characterisation of Sodium fluoroantimonate single crystals*, Ph.D. Thesis, Anna university, Madras, India -1992.
- [10]. J.Benet Charles, *Microindentation of analysis of Sodium fluoroantimonate crystals*, *Materials Chemistry and Physics* (1999) 99
- [11]. J.Benet Charles, F.D.Gnanam, *Cryst.Res.Technol.*, 25 (1990) 1063 - 1068.
- [12]. K.Sivakumar, J.Benet Charles and F.D.Gnanam, *Material Chemistry and Physics* 38 (1999) 337-341.
- [13]. J.Elsamma Chacko, J.Mary Linet, S.Mary Navis Priya, C.Vesta, B.Milton Boaz, S.Jerome Das, *Ind. J. Pure Appl. Phys.* 44(2006)260-263.
- [14]. P.Selvarajan, J.Glorium Arulraj, S.Perumal, *J.Crystal Growth* 311 (2009) 3835.
- [15]. R.Mary Jenila, T. R. Rajasekaran, J. Benet Charles, *Arch. Appl. Sci. Res.*, 2012, 4 (2012) 1850-1856.
- [16]. A.Szymanski, J.M. Szymanski, *Hardness estimation of materials: rocks and ceramic material*, PWN- Polish Scientific publishing, Warsaw (1989).
- [17]. K.V.Rao, A.A.Smakula, *J. Appl. Phys.* 36 (1965) 2031.
- [18]. P.Selvarajan, B.N.Das, H.B.Gon, K.V.Rao, *J. Mater. Sci.* 29 (1994) 4061.